EXPLORATION OF HIERARCHICAL LEADERSHIP AND CONNECTIVITY IN NEURAL NETWORKS IN VITRO

Michael I. Ham

Dissertation Prepared for the Degree of

DOCTOR OF PHILOSOPHY

UNIVERSITY OF NORTH TEXAS

December 2008

APPROVED:

Guenter. W. Gross, Co-Major Professor
Floyd. D. McDaniels, Co-Major Professor
Harris D. Schwark, Committee Member
Jacek Kowalski, Committee Member
Jannon L. Fuchs, Committee Member
Christopher Littler, Chair of the Department of Physics
Sandra L. Terrell, Dean of the Robert B. Toulouse School of Graduate Studies

Ham, Michael I. Exploration of hierarchical leadership and connectivity in neural networks in vitro. Doctor of Philosophy (Physics), December 2008, 27 pp., 3 tables, 22 illustrations, 68 titles.

Living neural networks are capable of processing information much faster than a modern computer, despite running at significantly lower clock speeds. Therefore, understanding the mechanisms neural networks utilize is an issue of substantial importance.

Neuronal interaction dynamics were studied using histiotypic networks growing on microelectrode arrays in vitro. Hierarchical relationships were explored using bursting (when many neurons fire in a short time frame) dynamics, pairwise neuronal activation, and information theoretic measures. Together, these methods reveal that global network activity results from ignition by a small group of burst leader neurons, which form a primary circuit that is responsible for initiating most network-wide burst events. Phase delays between leaders and followers reveal information about the nature of the connection between the two. Physical distance from a burst leader appears to be an important factor in follower response dynamics. Information theory reveals that mutual information between neuronal pairs is also a function of physical distance. Activation relationships in developing networks were studied and plating density was found to play an important role in network connectivity development. These measures provide unique views of network connectivity and hierarchical relationship in vitro which should be included in biologically meaningful models of neural networks.

ACKNOWLEDGMENTS

I would like to thank the people who have supported me through this process. Specifically, my mentor Dr. Guenter Gross who taught me how to perform electrophysiology experiments and introduced me to neuroscience. I would also like to thank Dr. Luís Bettencourt for his patience, support and introducing me to concepts of network interaction that I have found extremely interesting and useful. My sincere thanks to Dr. Floyd McDaniel for assisting me through this process. I am deeply appreciative of my committee members, Dr. Harris Schwark, Dr. Jannon Fuchs, and Dr. Jacek Kowalski, for the (nearly) thankless job of providing assistance with my dissertation.

Special thanks to my friends, Lucas Phinney, Mangal Dhoubadhal, Daniel Henry, David McNeil, Hillary Carter, Gary Carter, Vadas Gintautas, Humberto Godinez, Tom Lockard, Cody McElroy and Sasha Gutfraind for providing timely support and distractions when I needed them.

My family has been instrumental in this process, and I would like to thank my mom for supporting all of my decisions, my dad for encouraging me to go to college, my sister Laura for helping me through my first years of college, my sister Liz for her outlook on life, my brother Kenny for bouncing ideas off of me and providing interesting insight. To my grandparents I am deeply appreciative, I could not have accomplished this without both the monetary support and most importantly the encouragement they offered.

I would also like to thank Al and Carolyn Kinney for their support and Tiffany Kinney for encouraging me to continue on in my graduate work and for being supportive even during unusual circumstances.

Most importantly, I would like to thank my fiance Lissie Janszen for being incredibly understanding and putting up with me throughout this process.

CONTENTS

LIST OF TABLES

LIST OF FIGURES

CHAPTER 1

INTRODUCTION

Parts of the introduction and the next chapter are published in a paper titled: *Spontaneous coordinated activity in cultured networks: analysis of multiple ignition sites, primary circuits, and burst phase delay distributions* in the Journal of Computational Neuroscience (2008), Vol 24 pages 346-357 authored by Michael I. Ham, Luís M.A. Bettencourt, Floyd D. McDaniel and Guenter W. Gross.

No neural system is completely absent of electrophysiological activity. The putative roles of such spontaneous dynamics, although still relatively poorly understood, range from synaptic development and maintenance [28, 24, 19, 3, 31] to anticipatory states (e.g. [32]) that help animals reach rapid decisions from limited sensory input. Understanding spontaneous activity and the patterns of interaction between neurons in circuits are, therefore, issues of substantial importance.

A large body of theoretical analysis and experimental data indicates that cortical neuronal networks growing on microelectrode arrays (MEAs, Fig 1.1) *in vitro* provide useful experimental models of neural assembly (e.g. [9, 30, 4]) despite obvious limitations inherent to extrapolations from *in vitro* to *in vivo* systems (see for e.g. [6, 23]).

1.1. Burst Initiation

Collective high frequency action potential discharges are major features of *in vitro* networks [10, 22, 17, 18, 35, 8, 21, 2, 34, 33]. These periods of activity are termed network bursts and can influence learning and information processing by changing synaptic properties [5, 1]. Here, an extensive quantitative analysis of patterns of network burst initiation in cortical neural networks *in vitro* is performed.

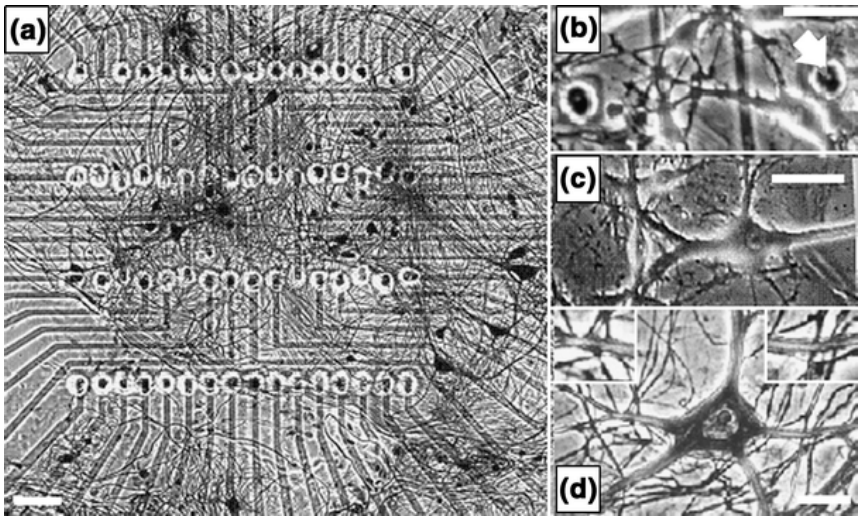

Figure 1.1. Neuronal networks in cell culture. (A) Network on a 64-electrode recording matrix. The transparent indium-tin oxide conductors are 8 μm wide and 1000$\mathring{A}$ thick. (92 days in vitro; Bodian stain Bars: 40 μm). (B-C) Living neurons on MEAs (phase contrast; bars: 40 μm). Gold-plated exposed ITO conductors are shown by arrows in (B). Transparent indium-tin oxide (ITO) conductors allow extensive optical access to the network morphology. (D) Single neuron showing synaptic profiles, enlarged in inserts (bar: 20 μm, neurofilament antibody stain). Image courtesy CNNS archive and previously published in [16].

Previous theoretical and experimental research showed that multiple ignition sites, sometimes termed initiation loci [22], nacelles [15], privileged neurons [11], and even initiation zones [12], create network bursts by recruiting constituent neurons. However, to date, very little has been done towards quantifying network initiation patterns resulting from such burst leader sites. Here, temporal relationships between leader (first spike in the network burst) and follower neurons are used to reconstruct network relationships amongst recorded neurons using a first-spike-in-burst analysis model. The model provides a unique view of network activation dynamics where neuronal firing is the result of network rather

than internal influences. This methodology also identified changes in network ignition site statistics after disinhibition with the $GABA_A$ blocker bicuculline. Extrapolation of these distributions produced minimum response delays, which are then used to estimate the distance, in terms of number of synapses, between neurons.

1.2. Identification of Functional Structures With Information Theory

Spike train data obtained from neural recordings are challenging to analyze because they display strong temporal stochasticity. Therefore, a probabilistic description of their time series in terms of active spiking periods and silence has been adopted as a standard decomposition of such data [29, 26] which can then be analyzed via information theory. Information theory reveals how the activity of one cell informs about the state of others and their relative informational configuration can be reconstructed. Examining all possible informational ensemble configurations provides a picture of the processing structures present in these small networks *in vitro*

1.3. Development of Functional Structures in Neural Networks

Dissociated networks are formed when brain tissue from prenatal mice is removed and mechanically and enzymatically dissociated and placed into culture. This tissue forms new connections and develops into a mature network with hundreds to thousands of synaptic connections per neuron. Action potential activity appears to play an important role in forming network connections [3, 13], but the exact mechanisms and informational relationships that form during development are relatively unknown.

Here the development of functional pairwise and informational relationships are examined in densely and sparsely seeded networks. Pairwise relationships in dense and sparse cultures are examined using a first response model. Resulting connectivity graphs are analyzed using a link entropy measure. Dense networks are seen to form strong early pairwise connections that equalize with most other neurons during maturation and results in high

link entropy. Sparse networks are slower to form connections and connections that do form are more unbalanced and have lower link entropy. Link entropy values are correlated to informational relationships which are unique for dense and sparse networks.

These approaches provide new statistical views of functional connectivity between neurons and several general quantitative characterizations of the internal dynamics of living cortical networks that should be reproduced in models of small to medium sized neural networks.

CHAPTER 2

BURST LEADERS AND NETWORK HIERARCHY

2.1. Burst Leaders

Cortical neural networks *in vitro* and *in vivo* exhibit coordinated periods of high frequency spike activity (Fig 2.1). Neuronal participation in such global activity events is the product of a chain reaction originating from an initiation site, or the burst leader [16].

Burst leaders likely belong to a small group of neurons with high levels of sub-threshold activity which occasionally rises above threshold and trigger spiking among closely coupled neurons [15]. Here the phenomenon of network burst activation is explored by studying the relationships between burst leaders and followers.

2.2. Major Burst Leaders, Response Delay Distributions and Network Delay Distributions

For detailed statistical analysis we define major burst leaders (MBLs) as neurons that lead at least 4% (arbitrarily set) of all network bursts (Fig 3). We define a response delay as the time between MBL onset and a follower's first spike. To be included in our statistical treatment, response delays must occur within 100 ms, which is commensurate with the duration of the network burst initiation period [11]. Response delay distributions (RDDs) were created for MBL/follower pairs via normalized (by number of network bursts associated with the MBL) frequency histograms, in 1 ms time bins, over ensembles of burst events. When MBLs did not lead they were considered followers. Combining all RDDs for different followers with the same MBL and normalizing the resulting distribution generates an MBL's network delay distribution. We analyze three different features of RDDs: 1) Peak delay: the delay time corresponding with the peak of the distribution. 2) Paired response correlations (PRCs): which measure the follower's participation (range 0 - 100%)

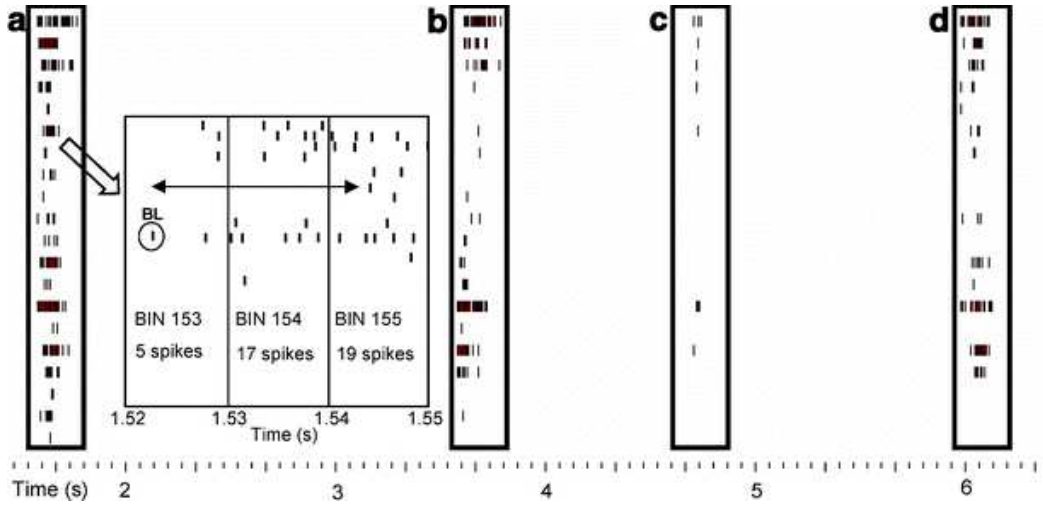

Figure 2.1. Raster displays of 20 frontal cortex units participating in coordinated bursting. Three network bursts (Boxes a, b, d) and one aborted network burst (Box c) occur during the first 6 seconds of recorded activity. Inset depicts the first 30 ms of network burst 1. The first twelve units (from top to bottom) are shown. The burst leader (BL) and a response delay (double headed arrow) are depicted. The bin number and spikes per bin are indicated. Bin width is 10 ms. Figure previously published in [16].

in network bursts led by the MBL. 3) Minimum response delays (MRDs): which is the shortest time delay corresponding to 10% of the peak response frequency and represents the fastest time in which a signal can pass between the MBL and follower. MRDs of about 2 ms correlate to the minimum signal delay between mono-synaptically connected neuronal pairs ([25]; minimum delay 2 ms, avg delay 4 ms).

The data set for the reported results consists of ten frontal cortex cultures, eight of which were subjected to disinhibition with 40 μM of bicuculline after at least five hours of normal (native) activity (summarized in Table 2.1). Bicuculline is an antagonist of the $GABA_A$ receptor that blocks the hyperpolarization effect of GABA in a competitive manner [7] When applied to frontal cortex cultures in saturating concentrations (40-60

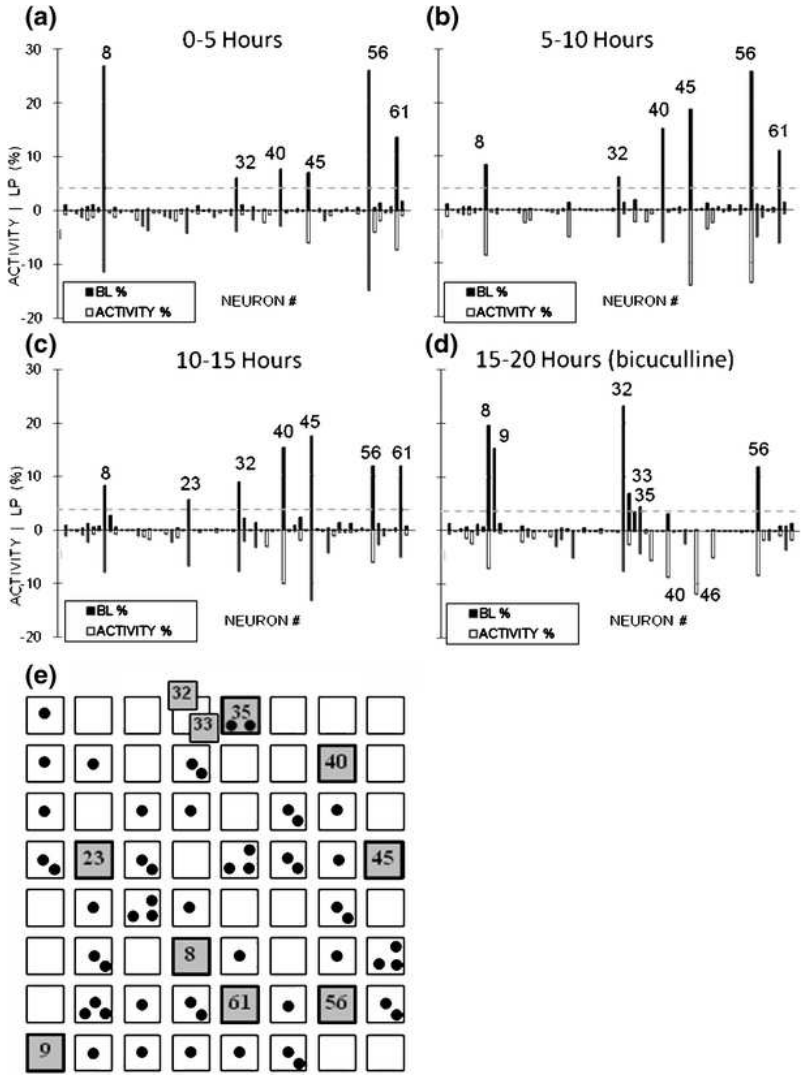

Figure 2.2. Burst leader probability (LP, positive) and percent spike activity (negative) for four consecutive 5 hr time periods (A-D). Dashed lines are MBL thresholds. In native activity (A-C), the pool of burst leaders is nearly constant, but the LPs changes. (D) Addition of 40 μM of bicuculline changes the burst leader pool. (E) Location of MBLs and followers on the 8 x 8 recording matrix (electrodes are separated by 150 μm). Numbers represent MBLs and dots show followers. Multiple dots and/or numbers per electrode represent the number of units monitored at that site. Figure previously published in [16].

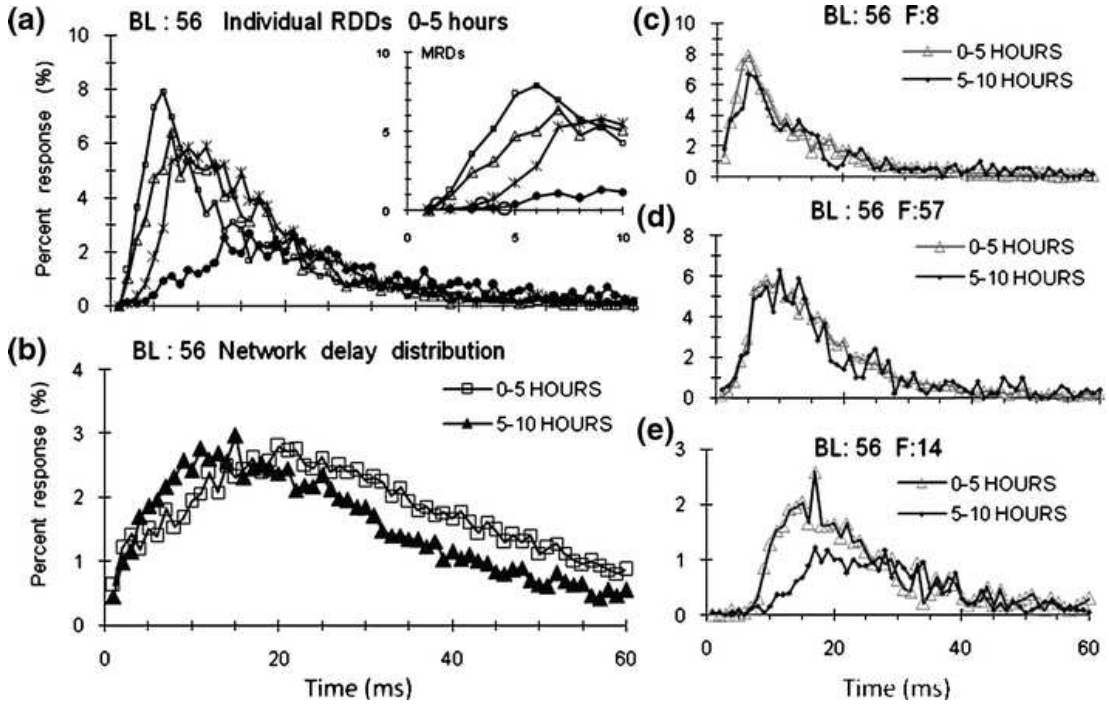

Figure 2.3. Examples of burst response delay distributions generated by the same burst leader. (A) RDDs of four different followers to BL 56. Each shows unique minimum response delays (MRDs), the fastest follower response time which is (inset, circles), and peak delays. (B) Network phase delay distributions (summation of all RDDs to BL 56) during two five hour periods. (C-E) Stability of individual RDDs during two consecutive five hour periods. MRDs and distributions remain similar. Data from network 1 (Table 2.1). Figure previously published in [16].

μM), it causes intensification and greater coordination of bursting with increased burst durations and average number of spikes in bursts [20, 27].

2.3. Burst Leader Characteristics

The 10 networks studied averaged approximately 1000 network bursts per hour. For an average of 42 discriminated units per culture (Table 2.1) this generates approximately 42,000 individual bursts/hour for analysis. Nearly all recorded neurons lead at least one

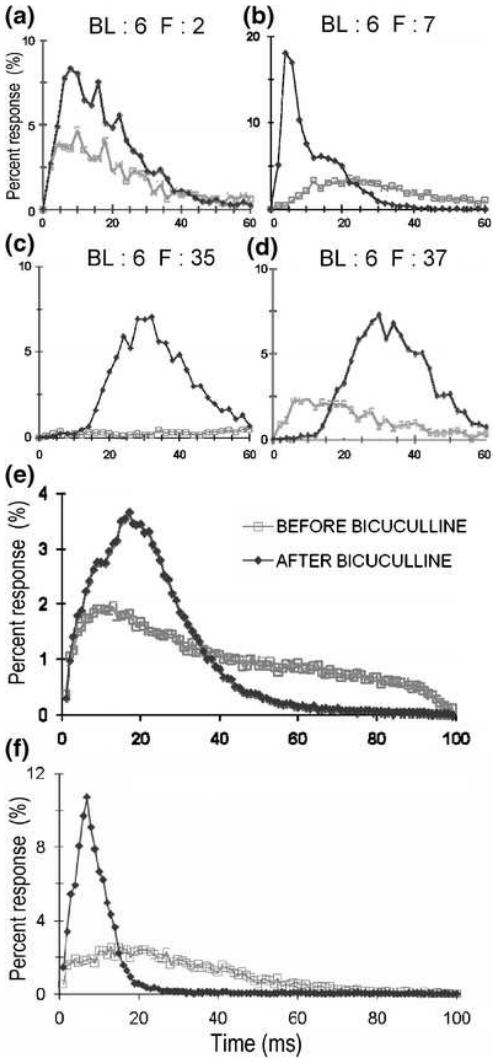

Figure 2.4. RDDs before (light lines) and after (dark lines) bicuculline addition. (A) Follower (F) 2 increases its responsiveness to burst leader (BL) 6, but maintains overall distribution shape. (B) F 7 respond faster and with greater precision to BL 6. (C) F 35 becomes more responsive to BL 6. (D) Conversely, F 37 responds later to BL 6. (E) NDD showing followers of BL 6 responding faster and with less variability after bicuculline. (F) NDD highlighting extensive distribution shift to shorter delays in response to bicuculline. Predominant effect of bicuculline is a shortening of phase delays and an increase in follower responsiveness. A-E : Network 2; F : Network 3. Figure previously published in [16].

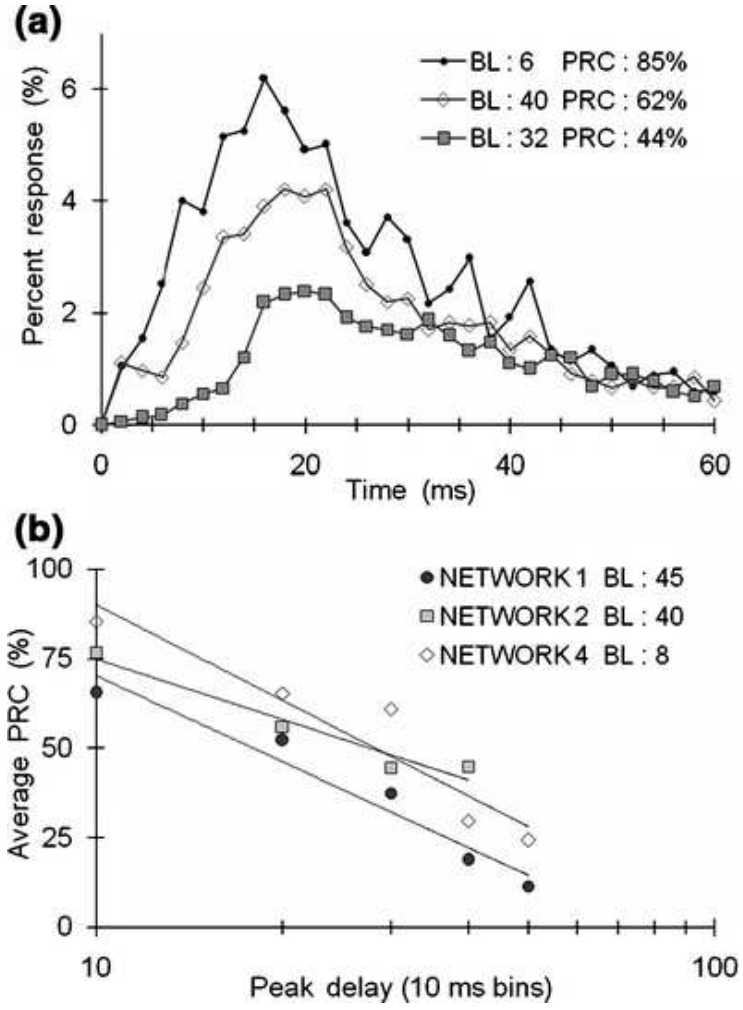

Figure 2.5. (A) RDDs of a single follower to three different burst leaders demonstrating unique influences of burst leaders on a single follower. In addition such pairs also have unique response correlations (PRCs) (B) PRC as a function of peak delays (10 ms bins) showing that strong correlations are associated with short peak delays. Logarithmic trend lines. Figure previously published in [16].

network burst per hour, but only a small subset of recorded neurons (average 17%; range 11-35%) were major burst leaders (MBLs, Table 2.1). Individually identified MBLs most likely belong to a small cluster of neurons, as suggested by Gross and Kowalski [15] and shown recently in unidimensional networks by Feinerman et al. [12]. MBLs statistically led

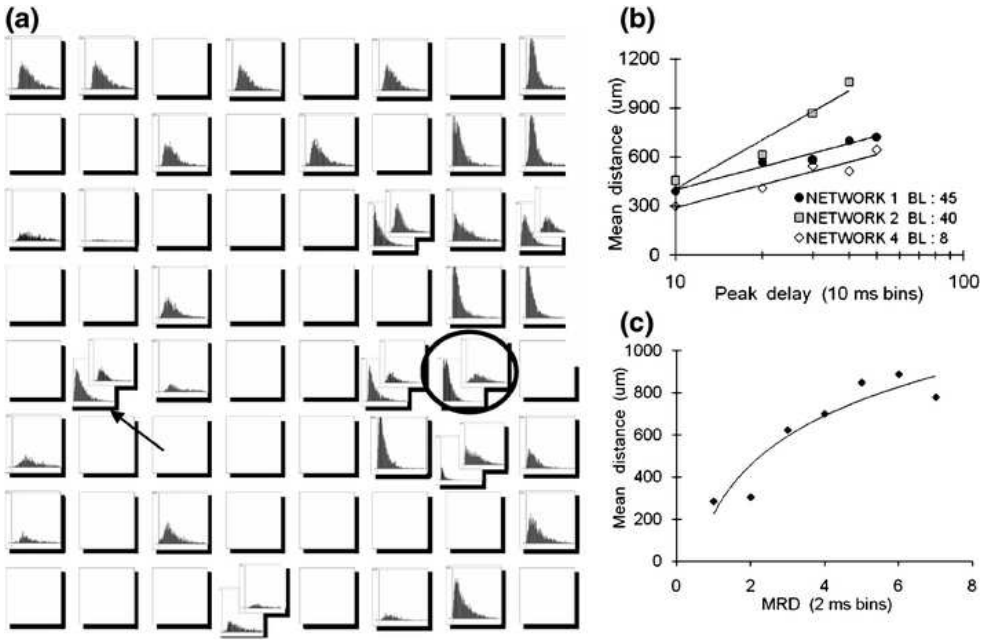

Figure 2.6. (A) RDDs for a burst leader (circled) are shown in their recording matrix location. It should be noted that the two distributions within the circle are follower neurons recorded on the same electrode. Multiple RDDs are depicted for electrodes with multiple units. Arrow points to the RDD of another MBL. Note small minimum response delay and high paired response correlation. (B) RDD peak delays in 10ms bins, plotted against the average physical distance from the burst leader. (C) Relationship between part A's MRDs (2 ms bins) and average distance. Logarithmic trend lines in B and C. Figure previously published in [16].

a similar amount of network bursts in normal medium (DMEM-5) and in medium containing the GABA channel blocker bicuculline (Table 2.1).

The set of MBLs remained approximately constant under native spontaneous activity conditions. Figure 2.2A-C shows native medium burst leadership statistics from network 1 during three consecutive five-hour recordings. Six neurons were MBLs during the first 10 hours (A&B), seven (previous six included) were major leaders during the third 5 hr

period (C), and six were identified after application of bicuculline (D). Under bicuculline, only three previous leaders, units 8, 32 and 56 remained, while three new leaders 9, 33 and 35 emerged. Note that identification numbers do not represent positions in the recording matrix. Actual leader locations on the matrix are shown in Fig 2.2E, which depicts an 8 x 8 microelectrode matrix with vertical and horizontal electrode separation of 150 μm. Shaded boxes represent MBLs with numbers corresponding to those in A-D. Followers are depicted by dots. It can be seen that the burst leader sites were distributed spatially over the entire matrix.

Burst leadership is not a direct function of neuronal spike rates. In Fig 2.2A-D, percent spike activity (number of individual spikes / total number of network spikes) is compared to burst leadership. During native activity, all MBLs had leadership percentages (positive bars) greater than percent spike activity (negative bars). Conversely many active spiking units showed no burst leadership beyond 1%, which we consider to be in the noise level. While MBLs typically exhibited a high percent spike activity, high activity did not ensure that a neuron would be an MBL.

2.4. Blockage of Inhibitory Synapses: Effects on MBL Pools

Loss of inhibition, induced by the application of 40 μM bicuculline, changes the makeup of the MBL group. Networks 1-8 (Table 2.1) had a total of fifty-two MBLs during native activity and forty-eight after bicuculline was added. Only twenty-five of the latter were present during native activity while the remaining twenty-three were new MBLs. In all networks, bicuculline also changed the form of the response delay relationships between neural pairs. Figure 2.4A-D show four examples of the observed effects bicuculline had on follower neuron responsiveness. (1) Increased responsiveness without major changes in distribution shape (2.4A); (2) shifting of distributions to shorter phase delays (2.4B), (3) participation by previously unresponsive neurons (2.4C). (4) distribution peak and the

			DMEM-5		+ 40μM Bicuculline	
N#	U#	Age	MBL	PNB	MBL	PNB
1	62	41	11	75	10	81
2	41	44	24	81	17	66
3	20	33	35	92	15	81
4	33	51	12	67	21	82
5	50	41	12	94	12	78
6	37	39	14	90	14	82
7	34	25	24	76	15	85
8	42	52	14	83	19	89
9	21	125	10	97	N/A N/A	
10	48	42	10	83	N/A	N/A
Means	42	48	17±3 (SD)	84±9.5	15±3.6	81±6.7

Table 2.1. Network features: N#: Network Number; U#: Number of units; MBL: MBLs as a percent of all units; PNB: Percentage of network bursts led by MBLs (%);

MRD shift to higher phase delays (2.4D). Overall, 51% of the MRDs shifted to shorter phase delays, while 19% shifted to longer MRDs and the remaining 30% showed no MRD change. There were no observed cases where the addition of bicuculline resulted in a follower becoming less responsive to a burst leader.

Such results show that studies of neural relationships and connectivity can be enhanced by specific pharmacological manipulations. An example is shown in Fig 2.4C where neuron 35 is unresponsive to MBL 6 in native medium. The addition of bicuculline resulted in strong responses by neuron 35 to burst leader 6. This indicated that, in the native state, inhibitory influences between 6 and 35 dominated, but excitatory connections existed. In future

experiments, pharmacological control over synaptic driving forces will become increasingly important in the quest for determination of functional connectivity.

Since each of the four bicuculline-induced RDD changes can happen to followers of the same burst leader (Fig 2.4A-D), observing the overall population effect requires examining the network delay distributions.

2.5. Network Delay Distributions

Network delay distributions (NDDs Fig 2.4E-F) are created by combining all individual response delay distributions that share a single major burst leader. These collective response patterns provide a view of network interaction with an MBL. NDDs are used to observe the effect of pharmacological manipulation on first-spike-in-burst relationships. In the NDD shown in Fig 2.4E, the bulk of network responses occurred earlier after the addition of bicuculline despite the peak delay increase. In this case, all response delays occurred within 70 ms whereas under native conditions, response delays up to 100 ms were observed. Figure 2.4F depicts a major population shift to shorter first-spike response times after the addition of bicuculline. Figure E and F are from network 1 and 2 (Table 2.1) respectively.

Blocking of inhibitory $GABA_A$ receptors with bicuculline did not have a universal effect on NDDs. In networks 1-5 (Table 2.1) there were a combined total of 33 MBLs during native activity. Of these, only 14 remained leaders after exposure to bicuculline. A comparison of these 14 network delay distributions in the native and bicuculline state revealed that peak delays of five shifted to the right, four shifted to the left and five showed no obvious change (Table 2.2). The distribution widths at half max for six network delay distributions expanded (average percent difference : 9), while seven compressed (average percent difference : 28). One showed no change. The changes in this parameter are network specific. Networks 2, 3, and 5 compress, but networks 1 and 4 expand. However, the predominant effect appears to be a tightening of the distribution width.

N#	MBL#	PDS	%dhm	%dpa	LPbb	LPab	%dLP
1	8	0	0	6	8	20	43
1	32	0	5	1	9	32	56
1	56	9	9	-4	12	12	0
2	6	4	-28	31	9	14	22
2	27	0	-16	18	6	10	25
2	29	0	-17	19	9	9	0
2	32	0	-16	19	13	7	-30
2	33	-3	-28	26	13	10	-13
3	7	-6	-61	61	14	22	22
4	3	14	8	-10	13	21	24
4	8	11	21	-17	32	12	-46
4	20	2	4	-15	18	21	8
4	24	-4	8	6	4	11	47
5	4	-16	-35	25	42	23	-29
Means		Neg: -7.3	Exp 7.9	Inc: 21.2	14.4	16	Inc: 30.7
		Pos: +4	Cmp: 28.7	Dec: 12			Dec: 29.4

Table 2.2. Network characteristics and changes induced by bicuculline. N#: Network Number; MBL#: Major burst leader number; PDS: Peak delay shift (ms); %dhm: % Diff in width at 1/2 max; %dpa: % Diff in peak amplitude; LPbb: Burst leadership percent before bicuculline; LPab: Burst leadership percent after bicuculline; %dLP: % Diff in burst leadership potential, Neg mean decrease, Pos mean increase, Exp Expansion of distribution (broadening), Cmp Compression of distribution (narrowing), Dec mean amplitude decrease (negative), Inc: mean amplitude increase (positive), Inc mean % increase in LP, Dec: mean % decrease in burst leadership potential

2.6. Paired Response Correlation and Peak Delays

Followers do not participate in every network burst event (Fig 2.1) and their RDDs are a function of the specific burst leader. To examine how often followers responded to MBLs we used a paired response correlation (PRC; Methods) scheme that ranged up to 100% and was unique for leader follower pairs. Distributions with PRCs less than 5% are in the noise level and such distributions were not used in any analysis dependent on PRCs. In Fig 2.5 we show RDDs, in 2 ms bins, generated by three MBLs acting individually on one follower with PRC values of 85, 62 and 44%.

In each of the 33 native medium MBLs in networks 1-5, average PRC values decreased as peak delays increased. Best logarithmic trend line fit (mean $R^2 = 0.78 \ \ 0.2$) occurred when followers of each MBL were grouped by peak delay into 5 or 10 ms bins and PRCs were averaged (Fig 2.5B). Such observations show that long peak delay times are associated with a lower probability of responding to a leader. It should be noted that PRCs were a function of the burst leader. Since long peak delays in these small networks most likely involve inhibitory synapses, this offers an explanation as to why removal of inhibition tends to increase PRCs, (Fig 2.4A-D) shorten peak delays (Fig 2.4B) and narrow distributions (Fig 2.4E-F). High PRCs combined with low MRDs and short peak delays indicate strong coupling between a leader/follower pair.

2.7. Distance and Response Delay Distributions

In many cases, a follower neurons physical distance from the burst leader appears to be a factor in the generation of its RDD. In 28 out of 33 MBLs in networks 1-5, large follower peak delays (10 ms bins) correlated to large average distances in the recording matrix. Figure 2.6A shows follower locations and RDDs for a single MBL (location circled). Most rapid responses occurred near the burst leader. It is important to stress that only the average distance increased with peak delay therefore exceptions could be found. For

example, an arrow points to a neuron relatively far from the burst leader (750 m), which had a short peak delay. Figure 2.6B shows three examples of the relationship between peak delay in 10 ms bins and average distance. A similar relationship was seen when minimum response delays were plotted against average distance. Figure 2.6C plots the MRDs from the data of 2.6A in 2 ms bins against the average distance per bin. It is likely that with increasing MRD and increasing distance, a larger number of serial synaptic steps are involved.

2.8. Network Connectivity

Morphological network circuitry is difficult to establish because many connections are made between neurons, even in widely distributed low density networks. This requires that emphasis be placed on functional connectivity to determine neuronal circuit structures. We hypothesize that the smallest delay between a leader follower pair, the MRD, can be used to approximate the minimum number of synaptic connections existing between the pair. A delay of 2 ms correlates to a mono-synaptic connection [25]. Similarly, a follower with a 4 ms response delay can be thought of as being 2 synapses away from the burst leader.

In Fig 2.7, we show followers grouped by their minimum response delays (in 2ms bins) to burst leaders 6 and 32 from the same network. Signals originating from different burst leaders did not activate followers in the same order. For example: when neuron 32 leads (Fig 2.7A), neuron 11 (arrow) is three bins away from neuron 5 (arrow). However, when neuron 6 leads (Fig 2.7B), they share the same bin. It should be noted that the first bin generally contained about half of the followers, and all other major burst leaders (grey squares). Neurons in this bin are thought to be in contact with the MBL through at least one single synapse connection. Hence, in the small networks analyzed, the majority of neurons have mono-synaptic connections to the major burst leaders.

Functional connectivity is also inferred using Paired Response Correlation (PRC) values. In Fig 2.8, connectivity in network 1 is examined using three different PRC thresholds (50, 70 and 90%). Directed graphs with edges connecting burst leaders (filled squares) to followers (white squares) meeting or exceeding the threshold were made. Dots represent followers with PRCs less than 50%. Figure 2.8 shows results from network 1 during hours 10-15 (2.2C). At 50% (Fig 2.8A), eleven neurons connected to each MBL. The majority of these highly connected neurons were also major burst leaders (8, 23, 32, 40, 45, 56, and 61). Altogether, nineteen out of 62 neurons responded (within 100 ms) to at least one major burst leader 50% of the time or higher. Each follower neuron connected to an average of 5.1 ± 2.1 MBLs. With a threshold of 70% (Fig 2.8B), six neurons, 23, 32, 40, 45, 56, and 61 (all MBLs), connected to each MBL. Twelve neurons remained connected at this level and each contacted an average of 4.52.0 MBLs. At a threshold of 90% (2.8C), one neuron (45) connected to all MBLs. A total of 8 neurons remained connected at this level, and each contacted an average of 2.8 ± 1.8 MBLs.

Figure 2.8C reveals a highly connected circuit of neurons. This circuit contained all of the major burst leaders, which, for this particular network, were responsible for initiating 75% of all network bursts. High connectivity between MBLs indicates that even if an MBL did not start a network burst, it was very likely to participate in that network burst and, presumably, help propagate the burst by recruiting closely coupled follower neurons. Similar findings were found in all study networks. RDDs where one MBL followed another MBL showed high levels of connectivity with MRDs around 2 ms and PRCs above 70%. Therefore, we conclude that this 'primary circuit,' composed mainly of MBLs, is responsible for the continual ignition of the network and generation of long-term spontaneous activity.

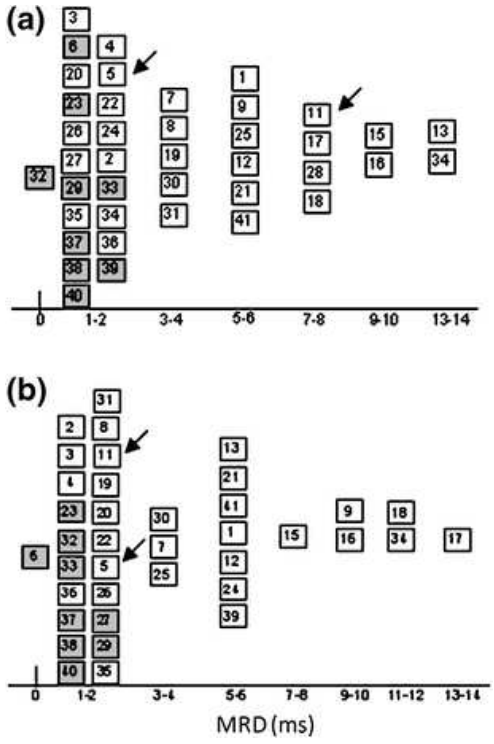

Figure 2.7. Minimum response delays can be used to determine network connectivity. (A) MRD pattern to burst leader 32. (B) MRD pattern to burst leader 6. Both are from the same network. Shaded boxes are major burst leaders. Burst leaders do not activate followers in the same order. Arrows show two followers with MRDs that vary by burst leader. The first two columns represent the same MRD time period. Figure previously published in [16].

2.9. Burst Leader Robustness

Burst leadership is unequally distributed. Very few neurons have levels of leadership large enough to be MBLs. However, inability to record from the entire body of neurons raises an important question about the burst leadership statistics presented earlier. Specifically, what would leadership statistics look like if all neurons could be recorded from?

To address this question, burst leader statistics are examined as if recorded neurons had been outside of the recording array. For a recording with N neurons, randomly selected

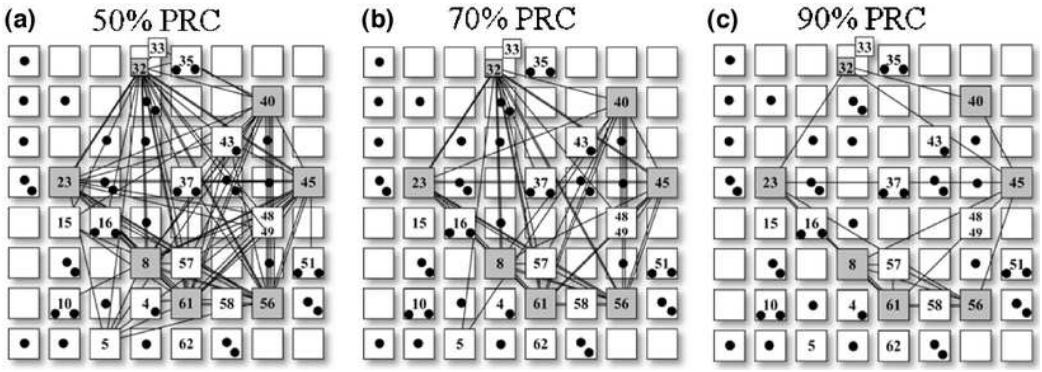

Figure 2.8. Pair-wise response correlations (PRCs) used to determine network connectivity. Burst leaders are shown with edges connecting to followers that exceed a PRC threshold of (A) 50% (B) 70% and (C) 90%. Filled squares are burst leaders; boxes with numbers are followers with at least one PRC value greater than 50%; dots are followers with PRCs less than 50%. Figure previously published in [16].

constituents are consecutively removed from the recording file and the resulting burst leadership statistics are calculated for the $N - k$ ($N > k > 0$) set of neurons. This random neuron removal test was run 100 different times and the average percent change in burst leadership for $N - k$ neurons was calculated and plotted as a function of neurons removed (solid line, Fig 2.9). This line is called a Lorenze curve and shows how leadership is distributed as k neurons are removed from the recording. The null model, where the leadership of each neuron removed is distributed evenly among the remaining neurons is plotted as a dashed line.

When neurons with large leadership (MBLs) are removed, their leadership is primarily distributed to other MBLs. This result supports the finding that burst leaders appear to act together as a primary circuit to ignite the network. If one of them were to no longer function, the others could act in a fault tolerant manner and continue to lead network bursts.

The area between the dashed line and the experimentally determined Lorenze curve can be examined using the Gini coefficient; $G = 1 - 2\int_0^1 L(X)dX$ where the Lorenz curve is represented by the function $Y = L(X)$. Gini coefficients range from 0, if the dashed line and the Lorenze curve are equal, to 1 if they are completely unequal.

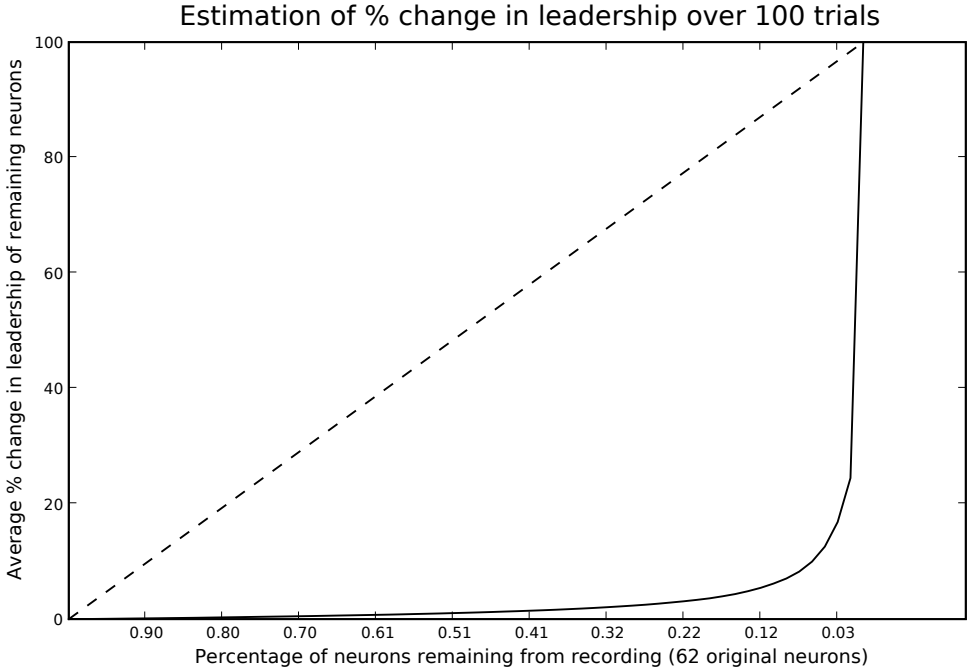

Figure 2.9. To test burst leadership distribution, randomly selected neurons are systematically removed and the average change in the remaining neurons burst leadership is shown (solid line). Dashed line represents the null model, where leadership is evenly distributed after a neuron is removed. Differences between the two curves give the Gini coefficient, a measure of inequality.

The experimentally determined Gini coefficient is .96 which indicates that burst leadership distributes very unequally among neurons.

This result suggests that if a new neuron were to be recorded, it is very unlikely to have much leadership. By extrapolation, it is reasonable to conclude that in the entire culture, only a small group of neurons lead a majority of the bursts. Therefore, despite the viewing

limitation imposed by microelectrode arrays, it is reasonable to assume that they provide a representative view of burst leader statistics.

2.10. Discussion

Major burst leaders are spontaneously active cells that play an important role in triggering network burst events and form a monosynaptically connected primary circuit. Together, burst leaders dominate the initiation of spontaneous network firing patterns via recruitment of other cells or cell clusters. Here, we explored three features of the activation mechanisms underpinning network bursts. First, major burst leaders (MBLs), which comprise a minority of cells in the network, form well-connected circuits with each other, and collectively lead most network bursts. Followers exhibit response delay distributions, paired response correlations, and minimum response delays unique to individual MBLs (Figs 2.3A, 2.7) suggesting that different MBLs will uniquely influence network information flow, information storage, its retrieval and responses to incoming sensory stimuli without modification to existing synaptic infrastructure. Second, detailed temporal lag relationships between MBL/follower pairs were characterized with response delay distributions (RDDs), which establish that responsiveness is a decreasing function of physical distance and number of synaptic connections between cells. RDDs have three important features: (1) minimum response delays (MRDs), which provide information about the minimum number of synaptic connections that exist between a leader/follower pair; (2) the paired response correlation (PRC), which represents a weighting factor for the connection between a leader/follower pair (see Fig 2.8 where PRCs were used to graph functional connectivity); and (3) the peak delay, which represents the delay time corresponding to the highest probability of follower response. Third, we showed that blocking $GABA_A$ inhibition narrows response delay distributions and results in drastic changes to the burst leader pool. The abruptness with which network activity changes after the addition of bicuculline suggests that existing network

circuitry, along with inherent conduction and synaptic delays remain unchanged while only computational (processing) activities are modified.

In approximately 18% of all cases, individual neurons increased their minimum response delay following the addition of 40 μM bicuculline (Fig 2.4C), a common concentration for pharmacological studies. This counterintuitive result might be explained by noting that 40 μM is not a saturating concentration. Therefore, some inhibitory circuitry could remain active and have greater inhibitory influence associated with increased firing rates. By acting on key connections, greater inhibition could increase minimum response delays or even expand network delay distributions (Table 2.2). While the primary effect remains a sharpening of the phase delay distributions, the effects of bicuculline concentration levels on population response dynamics warrants further study.

An issue common to all network wide measurements of neural activity, even in relatively small networks *in vitro*, is that present recording methods measure only a fraction of all activity. Recent research indicates that voltage sensitive dyes and optical recording methods are coming very close to revealing the activity of each individual network neuron [14, 12], but at this time electrophysiological recordings on microelectrode arrays (MEAs) still provide the best access to multiple individual neuronal signals with fine temporal resolution. Nevertheless, we estimate that data obtained from MEA recordings typically represents only about 5-10% of total neurons present and may be biased towards more active neurons and those that somehow project stronger signals. Therefore, the first neuron detected in a network burst could represent either a true ignition site or the fastest recorded follower of an ignition site outside the recording window. Despite this limitation, the identification of major burst leaders (MBLs) demonstrates that specific ignition sites are involved in generating spontaneous network activity.

Removing recorded neurons and analyzing the resulting burst leader statistics reveals that MBLs are a 'selfish group.' If they are removed from the recording, their burst

leadership is primarily transfered to other burst leaders, despite the fact that they are a minority. A large Gini coefficient shows that if any random neuron were selected for recording, it is unlikely to be a burst leader. This finding supports the idea that the limited recording window of a microelectrode array provides a representative picture of burst leader statistics.

Mechanisms similar to those creating strong basic driving forces in spontaneously active self-organized small networks *in vitro* are likely to be found in natural central nervous system activity. We hope that these quantitative characterizations of general collective spontaneous activity patterns *in vitro* will serve to guide and constrain future models and lead to greater understanding of the computational properties of nervous systems.

BIBLIOGRAPHY

[1] A. Artola and W. Singer. *NMDA receptors and developmental plasticity in visual neocortex. In: The NMDA receptor*. London: Oxford UP, 1994.

[2] J. M. Beggs and D. Plenz. Neuronal avalanches are diverse and precise activity patterns that are stable for many hours in cortical slice cultures. *J. Neurosci.*, 24:5216, 2004.

[3] Y. Ben-Ari. Developing networks play a similar melody. *Trends Neurosci*, 24:353–60, 2001.

[4] L. M. A. Bettencourt, G.J. Stephens, M.I. Ham, and G. W. Gross. Functional structure of cortical neuronal networks grown in vitro. *Phys. Rev. E*, 75:021915, 2007.

[5] T.V. Bliss and G.L.A Collingridge. A synaptic model of memory: long-term potentiation in the hippocampus. *Nature*, 361:31–39, 1993.

[6] M.A. Corner, J. Van Pelt, P.S. Wolters, R.E. Baker, and R.H. Nuytinck. Physiological effects of sustained blockade of excitatory synaptic transmission on spontaneously active developing neuronal networks?an inquiry into the reciprocal linkage between intrinsic biorhythms and neuroplasticity in early ontogeny. *Neurosci Biobehav Rev*, 26:127–185, 2002.

[7] D.R. Curtis, A.W. Duggan, D. Felix, and F.A.R. Johnston. Gaba, bicuculline and central inhibition. *Nature*, 226:1222–1224, 1970.

[8] P. Darbon, L. Scicluna, A. Tscherter, and J. Streit. Mechanisms controlling bursting activity induced by disinhibition in spinal cord networks. *Eur J Neurosci*, 15:671–683, 2002.

[9] T. B. DeMarse, D. A. Wagenaar, A. W. Blau, and S. M. Potter. The neurally controlled animat: Biological brains acting with simulated bodies. *Auton. Rob.*, 11:305, 2001.

[10] M.H. Droge, G.W. Gross, M.H. Hightower, and L.E. Czisny. Multielectrode analysis of coordinated, multisite, rhythmic bursting in cultured cns monolayer networks. *J Neurosci*, 6:1583–1592, 1986.

[11] D. Eytan and S. Marom. Dynamics and effective topology underlying synchronization in networks of cortical neurons. *J Neurosci*, 26:8465–8476, 2006.

[12] O. Feinerman, M. Segal, and E. Moses. Identification and dynamics of spontaneous burst initiation zones in unidimensional neuronal cultures. *J Neurophysiol*, 97(4):2937–2948, 2007.

[13] M.B. Feller. Spontaneous correlated activity in developing neural circuits. *Neuron*, 22:653–656, 1999.

[14] A. Grinvald and R. Hildesheim. Vsdi: a new era in functional imaging of cortical dynamics. *Nat Rev Neurosci*, 5:874–885, 2004.

[15] G.W. Gross and J.M. Kowalski. Origins of activity patterns in self-organizing neuronal networks in vitro. *J Intel Mater Syst Struct*, 10:558–564, 1999.

[16] M. I. Ham, L. M. A. Bettencourt, G.W. Gross, and F.D. McDaniel. Spontaneous coordinated activity in cultured networks: Analysis of multiple ignition sites, primary circuits, and burst phase delay distributions. *J. Comp. Neurosci.*, 24:346–357, 2008.

[17] Y. Jimbo, H.P.C. Robinson, and A. Kawana. Strengthening of synchronized activity by tetanic stimulation in cortical cultures: application of planar electrode arrays. *IEEE Trans Biomed Eng*, 45:1297–1304, 1998.

[18] Y. Jimbo, T. Tateno, and H.P.C. Robinson. Simultaneous induction of pathway-specific potentiation and depression in networks of cortical neurons. *Biophys J*, 76:670, 1999.

[19] L.C. Katz and C.J. Shatz. Synaptic activity and the construction of cortical circuits. *Science*, 274:1133–1138, 1996.

[20] E.W. Keefer, A. Gramowski, and G. W. Gross. Nmda receptor dependent periodic oscillations in cultured spinal cord networks. *J. Neurophysiol.*, 86:3030, 2001.

[21] X. Leinenkugel, R. Khazipov, R.C. Cannon, H. Hirase, Y. Ben Ari, and G. Buzsaki. Correlated bursts of activity in the neonatal hippocampus in vivo. *Science*, 296:2049–2052, 2002.

[22] E. Maeda, H. P. C. Robinson, and A. Kawana. The mechanisms of generation and propogation of synchronized bursting in developing networks of cortical neurons. *J. Neurosci*, 15:939, 1995.

[23] S. Marom and G. Shahaf. Development, learning and memory in large random networks of cortical neurons: lessons beyond anatomy. *Q. Rev. Biophys.*, 35:63, 2002.

[24] M. Meister, R.O.L. Wong, D.A. Baylor, and C.J. Shatz. Synchronous bursts of action potentials in ganglion cells of the developing mammalian retina. *Science*, 252:939–943, 1991.

[25] K. Nakanishi and F. Kukita. Functional synapses in synchronized bursting of neocortical neurons in culture. *Brain Res*, 795:137–146, 1998.

[26] I. Nemenman, W. Bialek, and R.R. de Rutyter Van Steveninck. Entropy and information in neural spike trains: Progress on the sampling problem. *Phys. Rev. E*, 69:05611, 2004.

[27] M. Puopolo and O. Belluzzi. Nmda-dependent, network-driven oscillatory activity induced by bicuculline or removal of mg2+ in rat olfactory bulb neurons. *Eur J Neurosci*, 13:92–102, 2001.

[28] R.R.Provine. Wing-flapping? develops in wingless chicks. *Behav Neur Biol*, 27:233–237, 1979.

[29] E. Schneidman, M. J. Berry II, R. Segev, and W. Bialek. Weak pairwise correlations imply strongly correlated network states in neural popula. *Nature*, 440:1007–1012, 2006.

[30] G. Shahaf and S. Marom. Learning in networks of cortical neurons. *J Neurosci*, 21:8782–8788, 2001.

[31] N.C. Spitzer. Electrical activity in early neuronal development. *Nature*, 444:707–712, 2006.

[32] Y. Takikawa, R. Kawagoe, and O. Hikosaka. Reward-dependent spatial selectivity of anticipatory activity in monkey caudate neurons. *J Neurophysiol*, 87:508–515, 2002.

[33] D.A. Wagenaar, J. Pine, and S.M. Potter. An extremely rich repertoire of bursting patterns during the development of cortical cultures. *BMC Neurosci*, 7:11, 2006.

[34] D.A. Wagenaar, M. Radhika, J. Pine, and S.M. Potter. Controlling bursting in cortical cultures with closed-loop multi-electrode stimulation. *J Neurosci*, 25:680–688, 2005.

[35] L.I. Zhang and M.M. Poo. Electrical activity and development of neural circuits. *Nat Neurosci*, 4:S1207–S1214, 2001.